The soluble glutathione transferase superfamily: Role of Mu class in Triclabendazole sulphoxide challenge in *Fasciola hepatica*

Rebekah B. Stuart[1,2], Suzanne Zwaanswijk[1], Neil D. MacKintosh[1], Boontarikaan Witikornkul[1], Mark Prescott[3], Peter M. Brophy[1] & Russell M. Morphew[1]

[1]Institute of Biological, Environmental and Rural Sciences, Aberystwyth University, Aberystwyth, Ceredigion, Wales. SY23 3DA

[2]Hybu Cig Cymru, Aberystwyth, Ceredigion, Wales. SY23 3FF.

[3]School of Biological Sciences, University of Liverpool, Liverpool, Merseyside, England, UK

Corresponding author: Dr R Morphew. Institute of Biological, Environmental and Rural Sciences (IBERS) Aberystwyth University, Aberystwyth, Wales. SY23 3DA.

Email: rom@aber.ac.uk

Tel: +44(0)1970 622314

Fax: +44(0)1970 622350

Running title: *F. hepatica* GST response to TCBZ-SO Treatment (46 characters)

Keywords: Proteomics; Affinity chromatography

Abstract

Fasciola hepatica (liver fluke), a significant threat to food security, causes global economic loss for the livestock production industry and is re-emerging as a food borne disease of humans. In the absence of vaccines the commonly used method of treatment control is by anthelmintics; with only Triclabendazole (TCBZ) currently effective against all stages of *F. hepatica* in livestock and humans. There is widespread resistance to TCBZ and detoxification by flukes might contribute to the mechanism. However, there is limited Phase I capacity in adult parasitic helminths and the major Phase II detoxification system in adults is the soluble Glutathione transferases (GST) superfamily. Previous global proteomic studies have shown that the levels of Mu class GST from pooled *F. hepatica* parasites respond under TCBZ-Sulphoxide (TCBZ-SO), the likely active metabolite, challenge during *in vitro* culture ex-host. We have extended this finding by using a sub-proteomic lead approach to measure the change in the total soluble GST profile (GST-ome) of individual TCBZ susceptible *F. hepatica* on TCBZ-SO-exposure *in vitro* culture. TCBZ-SO exposure demonstrated a FhGST-Mu29 and FhGST-Mu26 response following affinity purification using both GSH and S-hexyl GSH affinity resins. Furthermore, a low affinity Mu class GST (FhGST-Mu5) has been identified and recombinantly expressed and represents a novel low affinity mu class GST. Low affinity GST isoforms within the GST-ome was not limited to FhGST-Mu5 with second likely low affinity sigma class GST (FhGST-S2) uncovered through genome analysis. This study represents the most complete *Fasciola* GST-ome generated to date and has supported the sub proteomic analysis on individual adult flukes.

Introduction

Fasciolosis, caused by the trematode liver flukes *Fasciola hepatica* and *F. gigantica*, is a foodborne zoonotic affecting grazing animals and humans worldwide (Andrews 1999). Liver fluke cause economic losses of over US$3 billion worldwide per annum to livestock via a decrease in production of milk, meat and wool, susceptibility to other infections, condemnation of livers, and mortality (Boray 1997). There are no commercial vaccines as yet available with Triclabendazole (TCBZ) currently the most commonly used fasciolicide due to activity against both adults and juvenile stage fluke (Brennan, Fairweather et al. 2007). TCBZ is absorbed in the rumen and

passes through the blood to the liver where it is rapidly oxidised to the likely main active metabolites; Triclabendazole-sulphoxide (TCBZ-SO) (Alvarez, Solana et al. 2005) and Triclabendazole sulphone (TCBZ-SO_2) (Alvarez, Solana et al. 2005; Alvarez, Moreno et al. 2009). Unfortunately, TCBZ resistant liver fluke are wide spread, with resistance first encountered in Australia; but it is now evident in Western Europe (Brennan, Fairweather et al. 2007) including the UK (Thomas, Coles et al. 2000).

At present our understanding of the mode of action and detoxification of TCBZ is fragmented and mechanisms underpinning resistance may need to be resolved in order to measure early TCBZ resistance in populations and thus preserve efficacy (Brennan, Fairweather et al. 2007). To this end, the glutathione transferase (GST) superfamily have been identified as the major Phase II detoxification system present in all parasitic helminths. GSTs have been implicated in both drug metabolism and resistance in other groups of organisms e.g. insects and human tumours (Hayes and Pulford 1995). Eight cytosolic GST classes have been identified across kingdoms; namely Alpha, Mu, Pi, Sigma, Theta, Kappa, Zeta, and Omega (Cvilink, Lamka et al. 2009). In *F. hepatica* GSTs belonging to four classes have been revealed by biochemistry and bioinformatics; Omega (ω), Mu (μ), Sigma (σ) and Zeta (ζ) (Chemale, Morphew et al. 2006; Morphew, Eccleston et al. 2012). Chemale *et al*. (2010) further reported that Mu class GST levels vary, with Mu class GST-1 reduced in abundance while Mu class GST-26 increased in TCBZ resistant and susceptible *F. hepatica* under TCBZ sulphoxide (TCBZ-SO) exposure. In addition, Scarcella *et al.* (2012) identified that fluke resistant to TCBZ expressed significantly higher levels of GST activity compared to susceptible flukes. Furthermore, an amino acid mutation in Mu Class GST-26 has been linked to a TCBZ resistant liver fluke strain (Fernandez, Estein et al. 2015). However, to date, there has not been a robust sub-proteomic study that compared the expression of GST isotypes in individual liver fluke under TCBZ-SO stress. Thus, we purified GSTs from the cytosol of single adult flukes using a combination of Glutathione (GSH) and S-Hexyl-GSH agarose, resolved GST isotypes by 2-DE and identified individual GSTs by MS/MS with the support of genomic and transcriptomic databases. As a consequence we have identified a novel Mu, Sigma and Omega class GST designated FhGST-Mu5, FhGST-S2 and FhGST-O2 respectively. FhGST-Mu5 has been cloned and expressed in a recombinant and active form and characterised.

Materials and Methods

In vitro TCBZ culture

Individual liver fluke from natural infections were collected and exposed to TCBZ-SO as described previously (Morphew, MacKintosh et al. 2014). In brief, live adult *F. hepatica* were collected from a local abattoir (Randall Parker Foods, Llanidloes, Wales, UK) and washed in PBS at 37°C. Fluke were washed for 1 h with PBS replacement every 15 mins. Post-washes, replicates of 10 adult, sized matched, worms were placed into fluke Dulbecco's Modified Eagle Medium (DMEM) culture media containing 15 mM HEPES, 61 mM glucose, 2.2 mM Calcium acetate, 2.7 mM Magnesium sulphate, 1 µM serotonin and gentamycin (5 µg/ml) as previously described (Morphew, Wright et al. 2011). Flukes were maintained in culture at 37°C for 2 h (including transport to the laboratory) to establish a baseline protein expression profile. Upon completion of the initial 2 h incubation, culture media was replaced and supplemented with TCBZ-SO (LGC Standards, UK) at 50 µg/ml (Lethal dose) or 15 µg/ml (Sub-lethal dose) in DMSO (final conc. 0.1% v/v). For control samples only DMSO was added to a final volume of 0.1% v/v. Fluke cultures were then allowed to incubate at 37°C for a 6 h time period after which the media was refreshed, with DMSO and TCBZ-SO as required. Fluke cultures were incubated at 37°C for a further 6 h. A final refreshment of culture media was conducted and fluke cultures incubated for an additional 12 h at 37°C. Upon completion of the culture fluke were removed from the media and snap frozen individually in liquid N_2. All samples were stored at -80°C until required.

GST Assay and Purification

Individual adult *F. hepatica* were homogenised in an all-glass homogeniser on ice using 2 ml of lysis buffer containing 20 mM Potassium Phosphate pH 7.4, 0.1% v/v Triton-X 100 and EDTA-free protease inhibitors (Roche, Complete-Mini, EDTA-free). Samples were centrifuged at 100,000 x *g* for 45 minutes at 4^{o}C to obtain the supernatant, the cytosolic fraction. Protein levels were quantified by the method of Bradford (1976). GST enzymatic specific activity was determined according to the

conditions outlined by Habig *et al.* (1974) described previously (LaCourse, Perally et al. 2012) and stored at -80^{o}C until needed. Specific activity data was log_{10} transformed prior to statistical comparison carried out by a two way ANOVA.

Cytosolic proteins were applied to a GSH-agarose (Sigma-Aldrich) or an S-hexyl-GSH-agarose (Sigma-Aldrich) affinity matrix and purified at 4°C according to the manufacturer's instructions and as described previously (Morphew, Eccleston et al. 2012). Eluted proteins were concentrated using 10-kDa molecular weight cut off filters (Amicon Ultra, Millipore) and washed with ddH_2O. All samples were quantified again by the method of Bradford (Sigma-Aldrich).

Protein Preparation and 2-DE

IPG strips (7 cm, linear pH 3-10) were rehydrated with 100 µl of buffer (containing 8 M Urea, 2% w/v CHAPS, 33 mM DTT, 0.5% ampholytes pH range 3-10) plus 25 µl of sample protein and ddH_2O to load 20 µg of GSH or Hexyl-GSH affinity bound proteins. Samples were in-gel rehydrated for 16 hrs and isoelectrically focused on 7 cm pH 3-10 IPG strips to 10,000 Vh on a Protean® IEF Cell (BioRad). After focusing, strips were then equilibrated for 15 min in reducing equilibration buffer (30% v/v glycerol, 6 M urea, 1% DTT) followed by 15 min in alkylating equilibration buffer (30% v/v glycerol, 6 M urea, 4% iodoacetamide). IPG strips were run upon SDS PAGE (12.5% acrylamide) using the Protean® II 2-D Cell (BioRad). Gels were then Coomassie blue stained (Phastgel Blue R, Amersham, Biosciences), and imaged on a GS 800 calibrated densitometer (BioRad). Quantitative differences between 2-DE protein spots were analysed using Progenesis PG220, software version 200 (Nonlinear Dynamics Ltd.), using 5 biological replicates. Spots were automatically detected on gels and manually edited. Normalisation of spots was calculated using total spot volume multiplied by the total volume (Moxon, LaCourse et al. 2010). All gel images were warped using manual matching before average gels (5 gels were used to make the average gels) for each treatment group were produced. Unmatched protein spots were also detected on appropriate gel comparisons. Two-fold differences between protein spots with a $p<0.05$ were considered significant when average gels were compared.

Western Blotting

Following 2-DE, resolved proteins were transferred to nitrocellulose membranes. The nitrocellulose membrane was soaked in ddH_2O for 1 minute. The gel, membrane, filter paper and porous pads were equilibrated in 1X Western Blot Transfer Buffer (NuPAGE Transfer Buffer, Life Technologies) for 20 min.

Proteins were transferred at 40 V for 2 h in 1 X Western blot transfer buffer (50 ml NuPage transfer Buffer, 850 ml ddH_2O, 100 ml Methanol). To ensure proteins were transferred, the membrane was removed and stained with Amido black staining solution (0.1% w/v Amido black, 10% v/v Acetic Acid, 25% v/v isopropanol) for 1 min to detect the success of the transfer. The membrane was then washed with ddH_2O. The membrane was then placed in Amido black de-stain (25% v/v isopropanol and 10% v/v acetic acid) for 30 mins. The membrane was imaged using the GS-800 calibrated densitometer (BioRad). Amido black stain was removed with several washes of Tris buffered saline, 1% v/v Tween 20 (TTBS).

The nitrocellulose membrane was blocked in blocking buffer (TTBS + 5% milk powder) overnight. The membrane was then washed with TTBS and then incubated with the primary antibody for 1-2 h. A 1:5,000 dilution and a 1:30,000 antibody dilution in blocking buffer was used for anti-Mu and anti-Sigma GST respectively. After incubation with the primary antibody the membrane was washed in TBS for 10 min. The membrane was washed twice more before incubating with the secondary antibody (Anti-goat IgG raised in rabbits for the Mu and Anti-rabbit IgG raised in goats for the Sigma) for 1-2 hours at a 1:30000 dilution in blocking buffer. The membrane was then washed 3 times in Tris buffered saline (TBS). Interacting spots or bands were detected using the 5-Bromo-4-chloro-3-indolyl phosphate (BCIP) in conjugation with Nitro blue tetrazolium (NBT), according to manufactures instructions. To develop, a 1:2 solution of BCIP:NBT in substrate buffer consisting of 0.1 M tris, 100 mM NaCl and 5 mM magnesium chloride, adjusted to pH 9.5. To cease the over development, membranes were rinsed in ddH_2O. Blots were then scanned with a GS-800 calibrated densitometer (BioRad) and were imaged using Quantity One Version 4.6 software (BioRad, U.K.).

186 **Protein Identification**

187 Protein spots were manually excised from the gels and in-gel digested with trypsin
188 according to the method of Chemale *et al*. (2006). Tandem mass spectrometry
189 (MSMS) were performed according to the method described by Moxon *et al*. (2010).
190 Briefly, selected peptides from peptide digests were loaded onto a gold coated
191 nanovial (Waters, UK), and sprayed at 800 – 900 V at atmospheric pressure and
192 fragmented by collision induced dissociation using agron as the collision gas. Mass
193 Lynx v 3.5 (Waters, UK) ProteinLynx was used to process the fragmentation spectra.
194 Each fragmented spectrum was individually processed as follows; each spectrum
195 was combined and smoothed twice using the SavitzkyGolay method ± 3 channels,
196 background subtraction (polynominal order 15 and 10% below the curve). Each
197 spectrum was exported and spectra common to each 2-DE spot were merged into a
198 single MASCOT generic format (.mgf) file using the online peak list conversion utility
199 available at www.proteomecommons.org (Falkner, Falkner et al. 2007).

200

201 **Mass Spectrometry Database Analysis**

202 Merged files were submitted to MASCOT MSMS ion search set to search the
203 published *F. hepatica* genomes (Cwiklinski, Dalton et al. 2015; McNulty, Tort et al.
204 2017) using the webpage interface (MatrixScience). The following parameters were
205 selected for each peptide search; enzyme set at trypsin with one missed cleavage
206 allowed, fixed modifications set for carbamidomethylation with variable modifications
207 considered for oxidation of methionine, monoisotopic masses with unrestricted
208 protein masses were considered, peptide and fragment mass tolerance were set at ±
209 1.2 Da and 0.6 Da respectively for an ESI QUAD-TDF instrument (Moxon, LaCourse
210 et al. 2010).

211

212 ***In silico* investigation of *Fasciola* transcripts and *F. hepatica* genome**

213 Sequences representing known GST classes were obtained from NCBI
214 (http://www.ncbi.nlm.nih.gov/). A mammalian and a helminth GST sequence were
215 selected for each GST class where available. GST sequences were used to
216 tBLASTn the *F. hepatica* transcriptome (Young, Hall et al. 2010) and the *F. gigantica*
217 transcriptome (Young, Jex et al. 2011) both available to search at
218 (http://bioinfosecond.vet.unimelb.edu.au/wblast2.html). A second *F. hepatica*

transcriptome database (EBI-ENA archive ERP000012: an initial characterization of the *F. hepatica* transcriptome using 454-FLX sequencing) was also used to search against. *In silico* investigation of the known GST sequences and positive transcript hit were blasted against genome sequencing project of *F. hepatica* (Cwiklinski, Dalton et al. 2015). Transcript expression levels for individual GST isoforms were analysed from Cwiklinski *et al*. (2018). Each specific GST isoform was used to BLASTp the transcriptome to identify the respective expression level.

Cloning of newly identified genes

PCR amplification was carried out on an Applied Biosystems 96 Well Thermal Cycler. PCR of cDNA was performed using MyFi Taq (Bioline) following the manufacturer's instructions. Standard thermocycler conditions involved an initial denaturation at 95^{o}C for two minutes, followed by 25-35 cycles of denaturation (95^{o}C, 30 seconds), annealing (Gradient temperature specific for each gene of interest, 30 seconds) and extension (72^{o}C, 30-90 seconds), before a final extension at 72^{o}C for five minutes and holding period at 4^{o}C until products removed. Primers were based on the scaffolds from the *F. hepatica* genome (FhGST-S2 For: GGGCGATACTATCTATCAACGT Rev: GTGCGACTGACTTTGAATC; FhGST-O2 For: CACACAGCTGGAATTGA TTA Rev: TAATATTGACGGATCCAAACA). PCR products were ligated into pGEM-T-Easy, according to the manufacturer's protocol and sequenced in house. Sequences were translated using Expasy Translate (https://web.expasy.org/translate/) and molecular weight and pI calculated using Expasy Compute pI/Mw (https://web.expasy.org/compute_pi/). GST domains were predicted using PFam (El-Gebali, Mistry et al. 2019).

Protein sequence alignment and phylogenetic tree construction

All sequences were aligned using ClustalW through BioEdit Version 7.0.5.3 (10/28/05) (Hall 1999). To construct a phylogenetic tree an alignment of all GST sequences was exported into Molecular Evolutionary Genetics Analysis (MEGA) software version 4.0 (Tamura, Dudley et al. 2007). Analysis was performed using a neighbour-joining method, 1000-replicate, bootstrapped tree. The amino acid data were corrected for a gamma distribution (level set at 1.0) and with a Poisson correction.

253 **Recombinant *Fasciola hepatica* glutathione transferase Mu class (rFhGST-**
254 **Mu5) production**

255 FhGST-Mu5 was amplified via PCR using the following primer pair: rFhGST-Mu5
256 forward primer**, 5' CATATG**GCTCCAGTCTTA 3'; rFhGSTMu5 reverse primer, 5'
257 **GCGGCCGC**TTAACTGGGTGGTGCA 3' and a second reverse primer containing
258 the stop codon 5' **GCGGCCGC**ACTTTAACTGGGTGGTGCA 3'. Restriction enzyme
259 sites (in bold type and underlined) for NdeI (forward primer) and NotI (reverse
260 primer) were included so that the entire ORF could be directly cloned into the
261 pET23a (Novagen) vector. Recombinant proteins were produced in *Escherichia coli*
262 BL21 (DE3) cells (Bioline) as described previously (LaCourse, Perally et al. 2012;
263 Morphew, Eccleston et al. 2012).

264

265 *E.coli* preparations containing rFhGST-Mu5 were suspended in lysis buffer
266 (containing 5 mM MgCl, 400 mM NaCl and 20 mM sodium phosphate pH7.4) and
267 were lysed through a freeze/thaw method, freezing in liquid nitrogen followed by
268 thawing at 42°C three times. This was followed by 3 cycles of ultrasonication; the
269 samples were sonicated for 30 seconds with 30 second intervals in ice. The samples
270 were centrifuged at 13,200 x *g* for 20 minutes at 4°C. and purified by GSH-affinity
271 chromatography as described previously.

272

273 **Results**

274 **Limited induction of soluble *F. hepatica* GST by TCBZ-SO**

275 Prior to affinity chromatography GST enzymatic specific activity was assessed to
276 examine if overall cytosolic GST activity was induced by TCBZ-SO exposure (Table
277 1). In general, there was a trend to increased GST specific activity following
278 exposure to TCBZ-SO for treatment groups compared to controls (Supplementary
279 Figure 1). However, following ANOVA no significant difference was noted between
280 any of the treatment groups or the controls (2_{df}, F = 1.25, P = 0.320).

281

282

283 **GST proteomic profiling of individual fluke**

284 Two affinity matrices were then used to isolate GST isoforms from individual adult *F.*
285 *hepatica*. 18 individuals were homogenised independently and all 18 independently
286 processed through GSH or S-Hexyl GSH agarose columns to separate *F. hepatica*

GST proteins from other soluble proteins. Following purification, it was possible to compare the GST-ome from each individual *F. hepatica* exposed to TCBZ-SO, either a Sub-lethal concentration (15 µg/ml) or a Lethal concentration (50 µg/ml), versus those not exposed using 2-DE proteomics.

Proteomic arrays of the GSTs purified from S-hexyl GSH-agarose consistently yielded 13 protein spots (Figure 1A), whereas those purified from GSH-agarose column yielded 11 prominent protein spots (Figure 1B). All protein spots from both purification systems were confirmed as containing *Fasciola* GSTs using tandem mass spectrometry (Table 2; Full proteomic analysis Supplementary Table 1). Comparison of 2-DE protein arrays was then performed to establish if there was a change in abundance of the identified GSTs relating to the different treatment of TCBZ-SO (Figure 1C-F).

When comparing the S-Hexyl GSH Control array with both the S-Hexyl GSH TCBZ-SO exposed arrays it was noted that spot 14 (Figure 1A,C and E) was present on all Control arrays, thus present on the average Control array. However, the presence of this protein spot varied on the TCBZ-SO treatment arrays (Sub-lethal & Lethal). This particular protein spot was only present on 2 Sub-lethal arrays and 1 Lethal array. MSMS analysis identified this spot as Mu class GST29 (THD21358).

The comparison of the arrays produced via GSH agarose affinity columns identified two protein spots of interest when the average Control and average Sub-lethal arrays were examined with both spots increased in abundance in Sub-lethal samples; Spot 5, Mu class GST 26, (1_{df}, F = 3.89, P = 0.089) and Spot 7, Mu class GST 29, (1_{df}, F = 4.83, P = 0.064) both approaching statistical significance (Figure 1B and D; Supplementary Figure 2). No additional changes in protein abundance were observed for GSH purifications.

GST expression in the cytosol of individual fluke and affinity binding

Given the potential of Mu class GSTs responding to TCBZ-SO exposure, Western blotting was used to estimate the number of Mu class GSTs present in liver fluke cytosol prior to affinity chromatography, given previous indications that some GST

isoforms may fail to bind to affinity matrices (Brophy, Crowley et al. 1990). Assays were undertaken on five individual adult fluke using anti-*S. mansoni* Mu class polyclonal antibodies, previously shown to recognise *F. hepatica* Mu class GSTs (Chemale, Morphew et al. 2006). The anti-flatworm GST Mu class antibody recognised 8 GST subunits within the cytosolic profile (Figure 2A). Post purification the blot patterns display the same distinctive GST protein profiles following both GSH and S-Hexyl GSH affinity 2-DE gels (Figure 2B-C). A distinctive and reproducible 2-DE GST profile provides evidence that 8 GST subunits are recognized by the Mu antibody post purification.

Bioinformatic characterisation of GSTs identified in *F. hepatica*

Following analysis of available transcript and genome sequences the known 4 Mu class GSTs were identified alongside a fifth Mu class GST designated FhGST-Mu5. Following cloning and sequencing of FhGST-Mu5, multiple alignment of all Mu class GSTs of *F. hepatica* revealed the extent of identity and similarity across this class of GSTs (Figure 3A). Amino acid sequence similarity when comparing the newly identified FhGST-Mu5 (Genbank MT613329) with the previously known *F. hepatica* Mu class GSTs identified the closest sequence similarity was with FhGST-7 at approximately 54%. It is also worth noting that Genbank entry THD26413 matches to FhGST-Mu5 with 91.9% sequence identity but is an incomplete sequence lacking the N-terminus. When transcript expression was analysed for FhGST-Mu5 based on Cwiklinski *et al*. (2018), the levels of transcript within the adult is significantly lower than in alternative life cycle stages such as metacercariae and newly excysted juveniles from 1 to 24 h (Figure 3B).

Further transcript and genome investigation allowed the examination of the complete GSTome of *F. hepatica*. In addition to FhGST-Mu5, *in silico* investigation revealed the identification of a second Sigma class and a second Omega class GST. Bioinformatic characterization of the new FhGST-S2 and FhGST-O2 was undertaken to identify the structural features and characteristics of these genes/proteins. Only a single homologue for each was identified in the original *F. hepatica* genome. For FhGST-S2, gene BN1106_s1104B000225 (Scaffold 1104) was identified yet this is now fragmented and incomplete in the most recent version

of the genome (PRJEB25283) despite transcript support (Supplemental Table 2). For FhGST-O2, gene BN1106_s50B000678 (Scaffold 50) was revealed and is now designated as maker-scaffold10x_938_pilon-snap-gene-0.52/D915_03058. Each gene encoded for a predicted single protein isoform.

Both the newly predicted FhGST-S2 and FhGST-O2 were cloned (Supplemental Figure 3A) and sequenced. Confirmation of the correct class assignment was performed with multiple alignment (Supplemental Figure 3B and 3C) and comparison of gene intron exon structure (Supplemental Figure 4). Of note was a significant N-terminal extension of 20 amino acids in FhGST-S2 when compared to FhGST-S1. FhGST-O2 in comparison to FhGST-O1 revealed the addition of 1 amino acid to each of exons 1 and 5. Further confirmation of class assignment was support with both FhGST-S2 and FhGST-O2 subjected to a PFam domain analysis revealing key predicted GST features; FhGST-S2 with a predicted C-terminal domain (PFam GST_C_3) and FhGST-O2 with a predicted N- and C-terminal domain (PFam GST_N_3 and GST_C_2).

Following a full phylogenetic analysis of the completed *F. hepatica* GST-ome, all of the newly identified FhGST-Mu5, FhGST-S2 and FhGST-O2 were assigned to their respective clades (Figure 4). Of note is the close association of FhGST-Mu5 to the Schistosome Mu class GSTs rather than to the previously established four *Fasciola* Mu class isoforms.

Expression, purification and characterisation of rFhGST-Mu5

Full sequence length recombinant *F. hepatica* Mu class GST (rFhGST-Mu5) was expressed and purified from transformed *E.coli* cytosol following expression in BL21 (DE3) cells. Purity was assessed on SDS-PAGE gels (Figure 3C). Interestingly, rFhGST-Mu5 was not able to be produced as a pure protein with significant levels of contaminating *E. coli* proteins remaining in the sample following GSH affinity purification. However, rFhGST-Mu5 was produced as an active protein for further studies displaying enzymatic activity towards the model GST substrate 1-chloro-2,4-dinitrobenzene (CDNB). The specific activity for the rFhGST-Mu5 preparation was confirmed at 243.27 ± 92.45 nmol/min/mg.

Discussion

The 2-DE mapping of GSTs has been shown to be a useful tool to delineate the function of individual members of this soluble protein superfamily (Chemale, Morphew et al. 2006; Morphew, Eccleston et al. 2012), particularly as these proteins play a role in Phase II detoxification (Cvilink, Lamka et al. 2009). To date, research has only been completed on pooled cytosol samples from wild-type fluke and defined isolates and there has not been a robust sub-proteomic study that compared the expression of GST isotypes in individual fluke populations under TCBZ-SO challenge in culture. This study has adapted the pooled approach and, for the first time, performed analytical scale 2-DE mapping of GSTs from individual *F. hepatica* adult parasites. Thus, GSTs were purified from the cytosol of single adult flukes using either S-Hexyl Glutathione or Glutathione agarose columns, resolved using analytical 2-DE and identified individual GSTs by MSMS with the support of liver fluke transcriptomic and genomic databases. In doing so, we can identify individual fluke responses within the GST superfamily following exposure to chemotherapeutics. Furthermore, this finding has major implications for future population and resistance monitoring studies specifically on, but not limited to, liver fluke GSTs.

In the current study, both S-Hexyl GSH agarose and GSH agarose columns were used for GST purification at the individual fluke level. Previous studies (Chemale, Morphew et al. 2006; Morphew, Eccleston et al. 2012) have demonstrated that S-Hexyl GSH agarose columns have the ability to purify a greater range of GSTs in both *F. hepatica* and *F. gigantica* population mixes respectively thus was a useful inclusion in the current work at the individual fluke level. Using biochemical techniques and analytical sub-proteomics identified both Sigma and Mu class GSTs purified from individual adult *F. hepatica*. It was confirmed that both S-Hexyl GSH and GSH agarose columns have the ability to purify both Mu and Sigma class GSTs, but with GSH columns purifying the Sigma class to a much lesser extent expressing a preference to purify Mu class GSTs as observed for pooled samples (Chemale, Morphew et al. 2006).

The overall GST-ome profile, via GST activity and 2-DE arrays, demonstrated a general trend of response to TCBZ-SO exposure. Following exposure GST specific

418 activity increased with increasing TCBZ-SO concentration. In addition, the only
419 changes noted in both S-Hexyl GSH and GSH agarose purifications were recorded
420 abundance changes associated with Mu class GSTs, specifically FhGST-Mu29 and
421 FhGST-Mu26. Therefore, from activity data and proteomic profiling, it is likely that,
422 of the two GST classes identified, Mu class GSTs are likely highly important for
423 xenobiotic detoxification with Sigma class GSTs acting as secondary xenobiotic
424 sequesters with a primary role as a house-keeping enzyme and as, more
425 importantly, an immunomodulatory (LaCourse, Perally et al. 2012). This finding of
426 Mu class GST-TCBZ-SO detoxification supports the work of Chemale *et al*. (2010)
427 examining the TCBZ-SO response of TCBZ-resistant and TCBZ-susceptible
428 isolates. In this case, both FhGST-Mu29 and FhGST-Mu26 responded to TCBZ-SO
429 exposure, in agreement with the current study. We identified changes in response to
430 TCBZ-SO exposure linked to dimer and monomer formation of FhGST-Mu29 and
431 differential purification of both using the two purification methods. S-hexyl GSH
432 purification was more efficient at purifying FhGST-Mu29 dimers compared to GSH
433 agarose purification. On exposure to TCBZ-SO a reduction in FhGST-Mu29 dimers
434 was observed with a corresponding increase in FhGST-Mu29 monomers purified
435 through GSH agarose. The novel dimer-monomer GST conformational switch might
436 reflect a new liver fluke mechanism in response to TCBZ-SO challenge. GSTs
437 normally function as dimers but active monomeric GSTs have been previously
438 identified in *F. hepatica* (Brophy et al., 1990).
439
440 In *F. hepatica* there are four recognised isoforms of Mu class GSTs i.e. FhGST-
441 Mu26, 27, 28 & 29 (alternatively called FhGST-Mu51, 47, 7 & 1) with a fifth identified
442 only through bioinformatics previously (Morphew, Eccleston et al. 2012), and now
443 cloned and expressed in the current work. Alongside the identification of FhGST-S1,
444 four of the five Mu class GST isoforms were identified in the samples examined in
445 the current study under TCBZ-SO stress. In previous proteomic studies the same
446 four classes have also been identified. However, the functional significance of
447 multiple Mu GSTs is as yet unknown. Multiple Mu class isoforms might relate to their
448 role in the protection of the parasite from various classes of xenobiotics derived from
449 the host bile environment (Brophy, Mackintosh et al. 2012). Specifically, the current
450 work supports a role for FhGST-Mu29 in TCBZ-SO response via conformational
451 changes as identified by evidence of altered in dimer/monomer ratios. Of interest,

452 based on transcriptome evidence of Cwiklinski *et al*. (2018) FhGST-Mu29 is
453 naturally the highest expressed Mu class GST in adult fluke. In addition, FhGST-
454 Mu26 ranks third in all Mu class GST expression (FhGST-Mu29 > Mu27 > Mu26 >
455 Mu5 > Mu28). Therefore, it is likely that these primary expressed GSTs are
456 important in binding xenobiotics with structures such as such as TCBZ-SO.
457
458 In many cases peptides belonging to different GSTs were identified in a single
459 protein spot providing the identification of multiple GST isoforms. As reported by
460 Chemale *et al.* (2006), this may result from spot overlapping in the 2-DE gels, as
461 proteins may have a similar p*I*, potential modifications and co-migration. Of note is
462 the failure to identify the fifth Mu class GST, FhGST-Mu5, despite overlapping GST
463 isoforms identified in multiple spots. Given a sequence similarity of 54% for FhGST-
464 Mu5 compared to FhGST-7 the failure to identify FhGST-Mu5 is unlikely to be from
465 miss assigning sequenced peptides to alternative Mu class GSTs and likely
466 represents low expression as evidenced from transcriptomics (Cwiklinski, Jewhurst
467 et al. 2018) or, given the poor affinity purification of FhGST-Mu5, non-binding to
468 affinity columns.
469
470 In an attempt to assess if FhGST-Mu5 was not identified in affinity purified samples
471 as a result of non-binding, *F. hepatica* cytosolic material was probed with anti-*S.*
472 *mansoni* Mu polyclonal antibodies and compared with the profiles obtained post
473 affinity purification. Given that the same repertoire of protein spots following Western
474 blotting was visualised on both cytosolic and affinity purified fractions, in addition to
475 FhGST-Mu5 recognition by anti-*S. mansoni* Mu (data not shown), it seems unlikely
476 that FhGST-Mu5 was missed in the affinity proteomics study. In addition, it seems
477 unlikely that FhGST-Mu5 was missed due to low expression in adults given the
478 identification of FhGST-Mu28 in the current work and in previous studies (Chemale,
479 Morphew et al. 2006). Thus, the potential exists that FhGST-Mu5 is a low affinity
480 isoform. In support, Brophy *et al*. (1990) proposed that an endogenous ligand
481 interacts with GSTs preventing GSTs binding to the affinity matrix generating a 'low
482 affinity' fraction. Therefore, general inhibitory binding factors are likely present in the
483 liver fluke cytosol and may be important in flatworm GST function.
484

Following the successful induction and expression of FhGST-Mu5 it is clear that 'low affinity' GSTs are produced within the GST-ome of *F. hepatica* yet not all GSTs fail to bind from potential inhibitory factors. GSH affinity purification of rFhGST-Mu5 resulted in low impure yields of recombinant protein and suggests that FhGST-Mu5 is a 'low affinity' isoform. Previous studies have all successfully used glutathione affinity chromatography for successful purification of native and recombinant GSTs (Chemale, Morphew et al. 2006; LaCourse, Perally et al. 2012; Morphew, Eccleston et al. 2012) yet failed to purify FhGST-Mu5. Thus, to determine if rFhGST-Mu5 is an isoform with 'low affinity' for glutathione the specific activity was determined with the model substrate CDNB (Habig, Pabst et al. 1974). The specific activity of rFhGST-Mu5 was significantly lower than that recorded for the previously known 4 Mu Class GSTs from *F. hepatica* (Salvatore, Wijffels et al. 1995; Kalita, Shukla et al. 2017). This lower affinity may be correlated with the lower sequence homology and the more distant grouping of FhGST-Mu5 in phylogenetic modelling aligning closer to schistosome Mu class GSTs rather than the previous four *F. hepatica* Mu class. Brophy *et al*. (1990) demonstrated that following chromatofocusing 95% of 'low affinity' GSTs were relieved of their inhibition and thus, based on current evidence, it is likely that FhGST-Mu5 could indeed be classed as a 'low affinity' Mu class GST as part of the remaining 5% of activity. Low GSH affinity most likely accounts for the previous lack of detection during affinity studies with the initial identification achieved through transcriptomic analysis (Morphew, Eccleston et al. 2012). Given that FhGST-Mu5 clustered with schistosome Mu class GSTs during phylogenetics it is possible that FhGST-Mu5 and schistosome Mu class GSTs perform similar roles within these fluke species.

The current study represents the first 2-DE profiling of TCBZ-SO exposed *F. hepatica* GSTs. However, TCBZ-SO stress in *F. gigantica*, and the resulting GST activity, has been previously investigated. Shehab *et al.* (2009) examined GST activities from crude homogenates of adult and juvenile *F. gigantica* exposed to TCBZ-SO concentrations. This research indicated that a significant increase in the level of GST was present, in both adult and juvenile flukes, after exposure to TCBZ-SO (Shehab, Ebeid et al. 2009). Such a significant increase in response to TCBZ-SO prior to affinity purification was not noted in the current research and may reflect important differences between *F. hepatica* and *F. gigantica* GST expression.

519 Nevertheless, the work of Shehab and colleagues further supports the role of Mu
520 class GST in TCBZ-SO detoxification.
521
522 The release of the genome assemblies of *F. hepatica* (Cwiklinski, Dalton et al. 2015;
523 McNulty, Tort et al. 2017) has allowed for further in-depth and complete investigation
524 of the GST-ome complement of this parasitic flatworm. Two new soluble superfamily
525 GSTs were identified; a second Sigma (σ) class and a second Omega (ω) class, on
526 original genes BN1106_s1104B000225 and BN1106_s50B000678 (scaffolds 1104
527 and 50, respectively). Both GSTs contained Pfam IDs for the respective GSTs and
528 both sequences where successfully amplified through PCR and sequence verified.
529 The predicted molecular weight of the sub-units of the newly identified Sigma and
530 Omega GSTs were shown to be 26 and 27 kDa respectively, and this is in general
531 agreement with known soluble GSTs that have a subunit mass of between 23 and
532 28 kDa with an average length of 220 amino acids (Torres-Rivera and Landa 2008).
533 Gene structure analysing introns and exons for both the newly identified Sigma and
534 Omega genes in comparison with the previously identified *F. hepatica* Sigma and
535 Omega supported the confirmation of GST class assignment.
536
537 Previous research has demonstrated that model organisms (humans and mice) both
538 encode for 2 Omega class GST genes which are widely expressed (Board 2011)
539 reflecting expression within *F. hepatica*, albeit human and mice omega GSTs
540 comprise of six exons (Board 2011) rather than 5 in *F. hepatica* omega class GSTs.
541 Interestingly, omega class GSTs have been linked with drug resistance in human
542 cancers (Townsend and Tew 2003) and Alzheimer's disease (Allen, Zou et al. 2012)
543 and thus may have some role in anthelmintic resistance or detoxification not yet
544 discovered.
545
546 Sigma class GSTs in *F. hepatica* were also initially identified by Chemale *et al.*
547 (2006). A recombinant form of *F. hepatica* Sigma class GST, FhGST-S1, has since
548 been produced and demonstrated to have multi-functional roles, including general
549 endogenous detoxification, and is strongly linked with prostaglandin synthesis and
550 the modulation of dendritic cell activity (LaCourse, Perally et al. 2012). Across
551 trematode species the exon-intron structure of Sigma class GSTs is conserved.
552 Recently, reports of 5 newly identified Sigma class GSTs from *Clonorchis sinensis*

553 consist of 4 exons akin to the two *F. hepatica* genes (Bae, Kim et al. 2016). It was
554 also noted that the final exon, exon 4, of Sigma GST genes in the gene predictions
555 of all the trematode species investigated by Bae *et al.* (2016) consisted of 225 bp;
556 this conservation of gene structure likely reflects conserved biological function. As
557 yet, proteomic investigations have not identified FhGST-S2 from adult flukes despite
558 their presence in adult transcriptomes. It is therefore likely that FhGST-S2 remains
559 part of the unbound fraction of the GST-ome; a likely 'low affinity' sigma class GST.
560
561 With a key role for GSTs in the detoxification of TCBZ demonstrated through
562 proteomic profiling it is now crucial to understand any involvement of GSTs in TCBZ
563 resistance. This is of particular importance given that Scarcella *et al.* (2012)
564 identified that fluke resistant to TCBZ expressed significantly higher levels of GST
565 activity compared to susceptible flukes. The authors suggest that under TCBZ-SO
566 exposure there is an increased requirement for Phase I detoxification of TCBZ-SO,
567 to the less effective TCBZ-SO_2, and thus also require increased Phase II
568 detoxification, principally from GSTs, to catalyse TCBZ intermediates. Given the
569 recent bioinformatics identification of a potential Cytochrome P450 (Cwiklinski,
570 Dalton et al. 2015), TCBZ-SO exposure is likely to stimulate this Phase I pathway
571 leading to an increased requirement for phase II GSTs. Therefore, profiling the
572 specific GST isoforms will give more insight into resistance mechanisms.
573

574 **Conclusions**

575 Glutathione transferases (GSTs) are a multi-gene family of ubiquitous multifunctional
576 proteins that are predicted to have major roles in detoxifying both endogenous and
577 exogenous toxins as part of the Phase II system. We have expanded the knowledge
578 on this important protein family in the parasitic flatworm *F. hepatica*. In doing so, we
579 have revealed novel GST members including 'low affinity' Mu and Sigma class
580 enzymes. In addition, it is clear that GSTs respond to TCBZ-SO exposure and the
581 role of GSTs in TCBZ resistance awaits further investigation. Finally, the ability to
582 incorporate individual fluke for proteomic and sub-proteomic studies has implications
583 for potential early TCBZ resistance monitoring in liver fluke populations.
584

585 **Acknowledgements**

The authors are grateful to Randall Parker Foods (Wales) for providing *F. hepatica* infected sheep livers. This work was supported by the Biotechnology and Biological Sciences Research Council through an IBERS PhD Scholarship award and through Innovate UK (Grant Number: 102108).

References

Allen, M., F. G. Zou, et al. (2012). "Glutathione S-transferase omega genes in Alzheimer and Parkinson disease risk, age-at-diagnosis and brain gene expression: an association study with mechanistic implications." Molecular Neurodegeneration **7**.

Alvarez, L., G. Moreno, et al. (2009). "Comparative assessment of albendazole and triclabendazole ovicidal activity on *Fasciola hepatica* eggs." Veterinary Parasitology **164**(2-4): 211-216.

Alvarez, L. I., H. D. Solana, et al. (2005). "Altered drug influx/efflux and enhanced metabolic activity in triclabendazole-resistant liver flukes." Parasitology **131**: 501-510.

Andrews, S. J. (1999). The life cycle of *Fasciola hepatica*. Fasciolosis. J. P. Dalton. Oxford, C. A. B. International**:** 1-30.

Bae, Y. A., J. G. Kim, et al. (2016). "Phylogenetic characterization of *Clonorchis sinensis* proteins homologous to the sigma-class glutathione transferase and their differential expression profiles." Molecular and Biochemical Parasitology **206**(1-2): 46-55.

Board, P. G. (2011). "The omega-class glutathione transferases: structure, function, and genetics." Drug Metabolism Reviews **43**(2): 226-235.

Boray, J. C. (1997). Chemotherapy of infections with fasciolidae. Immunology, pathobiology and control of Fasciolosis. J. C. Boray. New Jersey, MSD AGVET Rahway**:** 83-97.

Bradford, M. M. (1976). "Rapid and sensitive method for quantitation of microgram quantities of protein utilizing principle of protein dye binding." Analytical Biochemistry **72**(1-2): 248-254.

Brennan, G. P., I. Fairweather, et al. (2007). "Understanding triclabendazole resistance." Experimental and Molecular Pathology **82**(2): 104-109.

618 Brophy, P. M., P. Crowley, et al. (1990). "Detoxification reactions of *Fasciola*
619 *hepatica* cytosolic glutathione transferases." Molecular and Biochemical
620 Parasitology **39**(2): 155-162.
621 Brophy, P. M., N. Mackintosh, et al. (2012). "Anthelmintic Metabolism in Parasitic
622 Helminths: Proteomic Insights." Parasitology **139**(9): 1205-1217.
623 Chemale, G., R. Morphew, et al. (2006). "Proteomic analysis of glutathione
624 transferases from the liver fluke parasite, *Fasciola hepatica*." Proteomics
625 **6**(23): 6263-6273.
626 Chemale, G., S. Perally, et al. (2010). "Comparative Proteomic Analysis of
627 Triclabendazole Response in the Liver Fluke *Fasciola hepatica*." Journal of
628 Proteome Research **9**(10): 4940-4951.
629 Cvilink, V., J. Lamka, et al. (2009). "Xenobiotic metabolizing enzymes and
630 metabolism of anthelminthics in helminths." Drug Metabolism Reviews **41**(1):
631 8-26.
632 Cwiklinski, K., J. P. Dalton, et al. (2015). "The *Fasciola hepatica* genome: gene
633 duplication and polymorphism reveals adaptation to the host environment and
634 the capacity for rapid evolution." Genome Biology **16**.
635 Cwiklinski, K., H. Jewhurst, et al. (2018). "Infection by the Helminth Parasite *Fasciola*
636 *hepatica* Requires Rapid Regulation of Metabolic, Virulence, and Invasive
637 Factors to Adjust to Its Mammalian Host." Molecular & Cellular Proteomics
638 **17**(4): 792-809.
639 El-Gebali, S., J. Mistry, et al. (2019). "The Pfam protein families database in 2019."
640 Nucleic Acids Research **47**(D1): D427-D432.
641 Falkner, J. A., J. W. Falkner, et al. (2007). "ProteomeCommons.org IO Framework:
642 reading and writing multiple proteomics data formats." Bioinformatics **23**(2):
643 262-263.
644 Fernandez, V., S. Estein, et al. (2015). "A single amino acid substitution in isozyme
645 GST mu in Triclabendazole resistant *Fasciola hepatica* (Sligo strain) can
646 substantially influence the manifestation of anthelmintic resistance."
647 Experimental Parasitology **159**: 274-279.
648 Habig, W. H., M. J. Pabst, et al. (1974). "Glutathione S-transferases: the first
649 enzymatic step in mercapturic acid formation." Journal of Biological Chemistry
650 **249**(22): 7130-7139.

651 Hall, T. A. (1999). "BioEdit: a user-friendly biological sequence alignment editor and
652 analysis program for Windows 95/98/NT." Nucleic Acids Symposium Series
653 **41**: 95-98.
654 Hayes, J. D. and D. J. Pulford (1995). "The glutathione S-Transferase supergene
655 family: Regulation of GST and the contribution of the isoenzymes to cancer
656 chemoprotection and drug resistance." Critical Reviews in Biochemistry and
657 Molecular Biology **30**(6): 445-600.
658 Kalita, J., R. Shukla, et al. (2017). "Comprehensive analysis of the catalytic and
659 structural properties of a mu-class glutathione s-transferase from *Fasciola*
660 *gigantica*." Scientific Reports **7**.
661 LaCourse, J. E., S. Perally, et al. (2012). "The Sigma Class Glutathione Transferase
662 of the Liver Fluke *Fasciola hepatica*." Plos Neglected Tropical Diseases **5**(1):
663 e937 . doi:910.1371/journal.pntd.0000937.
664 McNulty, S. N., J. F. Tort, et al. (2017). "Genomes of *Fasciola hepatica* from the
665 Americas Reveal Colonization with *Neorickettsia* Endobacteria Related to the
666 Agents of Potomac Horse and Human Sennetsu Fevers." Plos Genetics
667 **13**(1).
668 Morphew, R. M., N. Eccleston, et al. (2012). "Proteomics and *In Silico* Approaches to
669 Extend Understanding of the Glutathione Transferase Superfamily of the
670 Tropical Liver Fluke *Fasciola gigantica*." Journal of Proteome Research
671 **11**(12): 5876-5889.
672 Morphew, R. M., N. MacKintosh, et al. (2014). "*In vitro* biomarker discovery in the
673 parasitic flatworm *Fasciola hepatica* for monitoring chemotherapeutic
674 treatment." EuPA Open Proteomics **3**: 85-99.
675 Morphew, R. M., H. A. Wright, et al. (2011). "Towards Delineating Functions within
676 the *Fasciola* Secreted Cathepsin L Protease Family by Integrating *In Vivo*
677 Based Sub-Proteomics and Phylogenetics." Plos Neglected Tropical
678 Diseases **5**(1): e937. doi:910.1371/journal.pntd.0000937.
679 Moxon, J. V., E. J. LaCourse, et al. (2010). "Proteomic analysis of embryonic
680 *Fasciola hepatica*: Characterization and antigenic potential of a
681 developmentally regulated heat shock protein." Veterinary Parasitology
682 **169**(1-2): 62-75.

683 Salvatore, L., G. Wijffels, et al. (1995). "Biochemical analysis of recombinant
684 glutathione S-transferase of *Fasciola hepatica*." Molecular and Biochemical
685 Parasitology **69**(2): 281-288.
686 Scarcella, S., P. Lamenza, et al. (2012). "Expression differential of microsomal and
687 cytosolic glutathione-S-transferases in *Fasciola hepatica* resistant at
688 triclabendazole." Molecular and Biochemical Parasitology **181**(1): 37-39.
689 Shehab, A. Y., S. M. Ebeid, et al. (2009). "Detoxifying and Anti-Oxidant Enzmes of
690 *Fasciola gigantica* Worms Under Triclabendazole Sulphoxide (TCBZ-SX): An
691 *In Vitro* Study." Journal of the Egyptian Society of Parasitology **39**(1): 73-83.
692 Tamura, K., J. Dudley, et al. (2007). "MEGA4: Molecular Evolutionary Genetics
693 Analysis (MEGA) software version 4.0." Molecular Biology and Evolution
694 **Available online 10.1093/molbev/msm092.**
695 Thomas, I., G. C. Coles, et al. (2000). "Triclabendazole-resistant *Fasciola hepatica*
696 in southwest Wales." Veterinary Record **146**(7): 200-200.
697 Torres-Rivera, A. and A. Landa (2008). "Glutathione transferases from parasites: A
698 biochemical view." Acta Tropica **105**(2): 99-112.
699 Townsend, D. M. and K. D. Tew (2003). "The role of glutathione-S-transferase in
700 anti-cancer drug resistance." Oncogene **22**(47): 7369-7375.
701 Young, N. D., R. S. Hall, et al. (2010). "Elucidating the transcriptome of *Fasciola*
702 *hepatica* - A key to fundamental and biotechnological discoveries for a
703 neglected parasite." Biotechnology Advances **28**(2): 222-231.
704 Young, N. D., A. R. Jex, et al. (2011). "A Portrait of the Transcriptome of the
705 Neglected Trematode, *Fasciola gigantica*-Biological and Biotechnological
706 Implications." Plos Neglected Tropical Diseases **5**(2).

707

708

709

Figure 1: Representative 2-DE arrays of GSTs purified from *F. hepatica* using S-hexyl GSH and GSH agarose columns following TCBZ-SO exposure. A) S-hexyl GSH agarose purified GSTs from Control samples (TCBZ-SO 0 µg/ml). B) GSH agarose purified GSTs from Control samples (TCBZ-SO 0 µg/ml). C) S-hexyl GSH agarose purified GSTs from Sub-lethal samples (TCBZ-SO 15 µg/ml). D) GSH agarose purified GSTs from Sub-lethal samples (TCBZ-SO 15 µg/ml). E) S-hexyl GSH agarose purified GSTs from Lethal samples (TCBZ-SO 50 µg/ml). F) GSH agarose purified GSTs from Lethal samples (TCBZ-SO 50 µg/ml). All arrays were run on 7 cm IPG strips pH 3-10, 12.5% SDS PAGE and Coomassie blue stained. Spot numbers relate to GST putative identifications seen in Table 2.

Figure 2: Assessment of Mu class GST binding affinity through Western blotting of affinity purified GSTs comparison to cytosolic fractions. A) Visualisation of TCA precipitated cytosolic proteins of *F. hepatica* adult worms using two-dimensional gel electrophoresis (2-DE) and Western blot analysis probing for Mu class GSTs. In total, 100 µg of cytocolic protein was resolved on non-linear IPG strips and 12.5% polyacrylamide gels. B) and C) Visualisation of GSH agarose purified GST subunits of *F. hepatica* adult worms using two-dimensional gel electrophoresis (2-DE) and Western blot analysis analysis probing for Mu class GSTs. In total, 5 µg of GSH or S-Hexyl GSH purified GSTs were resolved on non-linear IPG strips and 12.5% polyacrylamide gels. A), B) and C) Western blots probed with anti-*S. mansoni* Mu antibody (1:5,000 dilution) and developed using alkaline phosphatase linked secondary antibody (anti-Goat IgG).

Figure 3. Bioinformatics, Expression and purification of recombinant rFhGST-Mu5. A) Multiple alignment of the 4 established *F. hepatica* Mu class GSTs and the newly identified FhGST-Mu5 revealed through transcriptome/genome analysis. No other Mu class GSTs were identified within the genome of *F. hepatica*. The consensus sequence SNAIL/TRAIL and their synonymous sequences in parasites are in the solid-line grey box. The residues forming the µ-loop are in dotted-line grey box. Arrowed are predicted GSH binding sites. Amino acid sequence identity of FhGST-Mu5 with the four previously known Mu class GSTs is provided at the end of the alignment. Accession numbers for each Mu class GST used: FhGST-Mu29/1 (P56598), FhGST-Mu28/7 (P31671), FhGST-Mu27/47 (P31670) and FhGST-

Mu26/51 (P30112). B) Transcript expression levels for FhGST-Mu5 were analysed from Cwiklinski *et al*. (2018). C) SDS-PAGE gel of the expression and purification of rFhGST-Mu. L: *E. coli* total cytosolic protein lysate, 10 µg. W1 and W2: Column washes removing non-binding proteins, 10 µl. FT: Flow through proteins collected after passing through a GSH-agarose column, 10 µg. E: Eluted GSH-affinity purified recombinant rFhGST-Mu5 protein, 2 µg. Run on 12.5% SDS-PAGE and Coommassie blue stained. Arrowed is the band representing rFhGST-Mu5.

Figure 4: Phylogenetic analysis of the soluble cytosolic GST superfamily. Neighbour-joining phylogenetic tree constructed using amino acid sequences through MEGA v 7.0 with 1000 bootstrapped support and a Poisson correction. All reported accession numbers are from Genbank. Where sequences were identified *in silico*, only contig numbers are reported. Those from *F. gigantica* were taken from the study of Young *et al*. (2011) and transcripts produced by Aberystwyth University. Those from *F. hepatica* were taken from the study of Young *et al*. (2010) and transcripts produced by the University of Liverpool (EBI-ENA archive ERP000012: An initial characterization of the *F. hepatica* transcriptome using 454-FLX sequencing).

764 **Table 1:** GST specific activity assays of *F. hepatica* GST samples exposed to
765 TCBZ-SO at Control (0 µg/ml), Sub-lethal (15 µg/ml) or Lethal (50 µg/ml) dose. Total
766 activity (nmol/min), total protein (mg) and specific activity (nmol/min/mg) are
767 included.

Treatment	Total activity (nmol/min).	Total protein (mg).	Specific activity (nmol/min/mg).
Control	4463.44	8.55	522.04 ± 77.92
Sub-lethal	6002.92	10.52	570.62 ± 190.46
Lethal	6190.82	9.35	662.12 ± 134.63

768

769

770 **Table 2.** Putative protein identification of GST isoforms from *F. hepatica* by MSMS.
771 Peptide sequences from spots trypsin digested were used to search against both *F.*
772 *hepatica* genomes for the identification of the specific members of the GST
773 superfamily. MASCOT ion scores of >42 indicate identity or extensive homology
774 ($p<0.05$). An accession number from Genbank relating to the top scoring BLAST hit
775 to determine GST isoform is also reported. Changes in abundance (↑ or ↓) are
776 denoted for spots responding to sub-lethal or lethal (SL or L) TCBZ-SO exposure for
777 either purification method (GSH or Hex-GSH).
778

Spot	Mascot Score	Genome Accession Number	Putative Identification	Total Peptides	Unique Peptides	Sequence Coverage	GST BLAST Accession Number	Fasciola GST Clade	Abundance Change
1	243	Maker-scaffold10x_490_pilon-snap-gene-0.8	Glutathione S-transferase protein	39	8	28.5	ADP09370	Mu 26/51	-
	216	D915_15048	Glutathione S-transferase protein	31	5	25.6	THD18760	Mu 27/47	
	209	Maker-scaffold10x_1184_pilon-snap-gene-0.31	Glutathione S-transferase protein	26	5	13	P31671	Mu 28/7	
	225	Maker-scaffold10x_1043_pilon-snap-gene-0.18	Glutathione S-transferase protein	21	5	26.9	ABI79450	S1	
	62	D915_11958	Glutathione S-transferase protein	16	8	28	TPP64849	Mu 29/1	
2	125	Maker-scaffold10x_490_pilon-snap-gene-0.8	Glutathione S-transferase protein	26	6	21.2	ADP09370	Mu 26/51	-
	105	D915_15048	Glutathione S-transferase protein	25	5	25.6	THD18760	Mu 27/47	
	100	Maker-scaffold10x_1043_pilon-snap-gene-0.18	Glutathione S-transferase protein	21	5	24.5	ABI79450	S1	
	173	D915_11958	Glutathione S-transferase protein	10	5	18	TPP64849	Mu 29/1	
	92	D915_13000	Glutathione S-transferase protein	9	2	12.4	THD20590	Mu 28/7	
	49	Maker-scaffold10x_61_pilon-snap-gene-0.52	Tubulin-tyrosine ligase family protein	3	2	4.8	-	-	
3	165	Maker-scaffold10x_490_pilon-snap-gene-0.8	Glutathione S-transferase protein	48	9	33.9	ADP09370	Mu 26/51	-
	154	Maker-scaffold10x_490_pilon-snap-gene-0.5	Glutathione S-transferase protein	34	5	31	P31670	Mu 27/47	
	79	D915_13000	Glutathione S-transferase protein	11	2	12.4	THD20590	Mu 28/7	
4	421	Maker-scaffold10x_490_pilon-snap-gene-0.8	Glutathione S-transferase protein	84	11	37.7	ADP09370	Mu 26/51	-
	346	Maker-scaffold10x_1184_pilon-snap-gene-0.31	Glutathione S-transferase protein	55	7	14.6	P31671	Mu 28/7	
	345	Maker-scaffold10x_490_pilon-snap-gene-0.5	Glutathione S-transferase protein	60	6	32.1	P31670	Mu 27/47	
	67	Maker-scaffold10x_2285_pilon-snap-gene-0.12	Glutathione S-transferase protein	6	3	16.8	THD21358	Mu 29/1	
5	1009	Maker-scaffold10x_490_pilon-snap-gene-0.8	Glutathione S-transferase protein	165	15	46.8	ADP09370	Mu 26/51	GSH SL ↑
	769	Maker-scaffold10x_1184_pilon-snap-gene-0.31	Glutathione S-transferase protein	114	12	26.5	P31671	Mu 28/7	
	859	Maker-scaffold10x_490_pilon-snap-gene-0.5	Glutathione S-transferase protein	111	9	47.1	P31670	Mu 27/47	
	128	D915_11958	Glutathione S-transferase protein	48	12	36.7	TPP64849	Mu 29/1	
	162	D915_13524	Hypothetical Protein	25	1	25	-	-	
	52	Maker-scaffold10x_1043_pilon-snap-gene-0.18	Glutathione S-transferase protein	5	3	15.6	ABI79450	S1	
	61	Maker-scaffold10x_61_pilon-snap-gene-0.52	Tubulin-tyrosine ligase family protein	3	2	5.5	-	-	
6	645	Maker-scaffold10x_1184_pilon-snap-gene-0.31	Glutathione S-transferase protein	113	12	28.9	P31671	Mu 28/7	-
	597	Maker-scaffold10x_490_pilon-snap-gene-0.8	Glutathione S-transferase protein	112	12	42.7	ADP09370	Mu 26/51	
	643	D915_15048	Glutathione S-transferase protein	90	9	34.4	THD18760	Mu 27/47	
	284	D915_11958	Glutathione S-transferase protein	55	12	34	TPP64849	Mu 29/1	
	54	Maker-scaffold10x_1043_pilon-snap-gene-0.18	Glutathione S-transferase protein	13	6	30.2	ABI79450	S1	
7	868	D915_11958	Glutathione S-transferase protein	177	19	55.7	TPP64849	Mu 29/1	GSH SL ↑
	203	Maker-scaffold10x_490_pilon-snap-gene-0.8	Glutathione S-transferase protein	64	11	34.2	ADP09370	Mu 26/51	
	210	Maker-scaffold10x_1184_pilon-snap-gene-0.31	Glutathione S-transferase protein	59	10	23.1	P31671	Mu 28/7	
	192	Maker-scaffold10x_490_pilon-snap-gene-0.5	Glutathione S-transferase protein	59	9	54.5	P31670	Mu 27/47	
	154	Maker-scaffold10x_1043_pilon-snap-gene-0.18	Glutathione S-transferase protein	15	7	46.2	ABI79450	S1	
8		No Significant hits							-
9	220	Maker-scaffold10x_1184_pilon-snap-gene-0.31	Glutathione S-transferase protein	49	11	23.1	P31671	Mu 28/7	-
	216	D915_15048	Glutathione S-transferase protein	43	8	35.6	THD18760	Mu 27/47	
	189	Maker-scaffold10x_2285_pilon-snap-gene-0.13	Glutathione S-transferase protein	35	7	34.8	THD20842	Mu 26/51	
	171	D915_11958	Glutathione S-transferase protein	32	11	31.7	TPP64849	Mu 29/1	
	53	Maker-scaffold10x_1043_pilon-snap-gene-0.18	Glutathione S-transferase protein	10	5	25.9	ABI79450	S1	-
10	115	D915_15048	Glutathione S-transferase protein	44	9	44.4	THD18760	Mu 27/47	
	106	maker-scaffold10x_1184_pilon-snap-gene-0.31	Glutathione S-transferase protein	36	6	13.7	P31671	Mu 28/7	
	66	D915_12658	Glutathione S-transferase protein	29	6	25.8	THD20842	Mu 26/51	
11	217	Maker-scaffold10x_1043_pilon-snap-gene-0.18	Glutathione S-transferase protein	28	7	33	ABI79450	S1	-
	100	maker-scaffold10x_490_pilon-snap-gene-0.8	Glutathione S-transferase protein	19	7	25.9	ADP09370	Mu 26/51	
	87	D915_13000	Glutathione S-transferase protein	8	2	12.4	THD20590	Mu 28/7	
12	302	Maker-scaffold10x_1043_pilon-snap-gene-0.18	Glutathione S-transferase protein	34	9	39.2	ABI79450	S1	-
	68	Maker-scaffold10x_2285_pilon-snap-gene-0.13	Glutathione S-transferase protein	8	2	10.3	THD20842	Mu 26/51	
	51	D915_13000	Glutathione S-transferase protein	4	1	7.1	THD20590	Mu 28/7	
13	439	Maker-scaffold10x_490_pilon-snap-gene-0.8	Glutathione S-transferase protein	86	14	39.2	ADP09370	Mu 26/51	-
	401	Maker-scaffold10x_1184_pilon-snap-gene-0.31	Glutathione S-transferase protein	63	13	26.2	P31671	Mu 28/7	
	419	Maker-scaffold10x_490_pilon-snap-gene-0.5	Glutathione S-transferase protein	63	8	47.1	P31670	Mu 27/47	
	111	Maker-scaffold10x_1043_pilon-snap-gene-0.18	Glutathione S-transferase protein	28	10	49.5	ABI79450	S1	
	130	D915_11958	Glutathione S-transferase protein	25	9	29.3	TPP64849	Mu 29/1	
14	98	Maker-scaffold10x_2285_pilon-snap-gene-0.12	Glutathione S-transferase protein	12	5	24.1	THD21358	Mu 29/1	Hex GSH SL↓ L↓↓

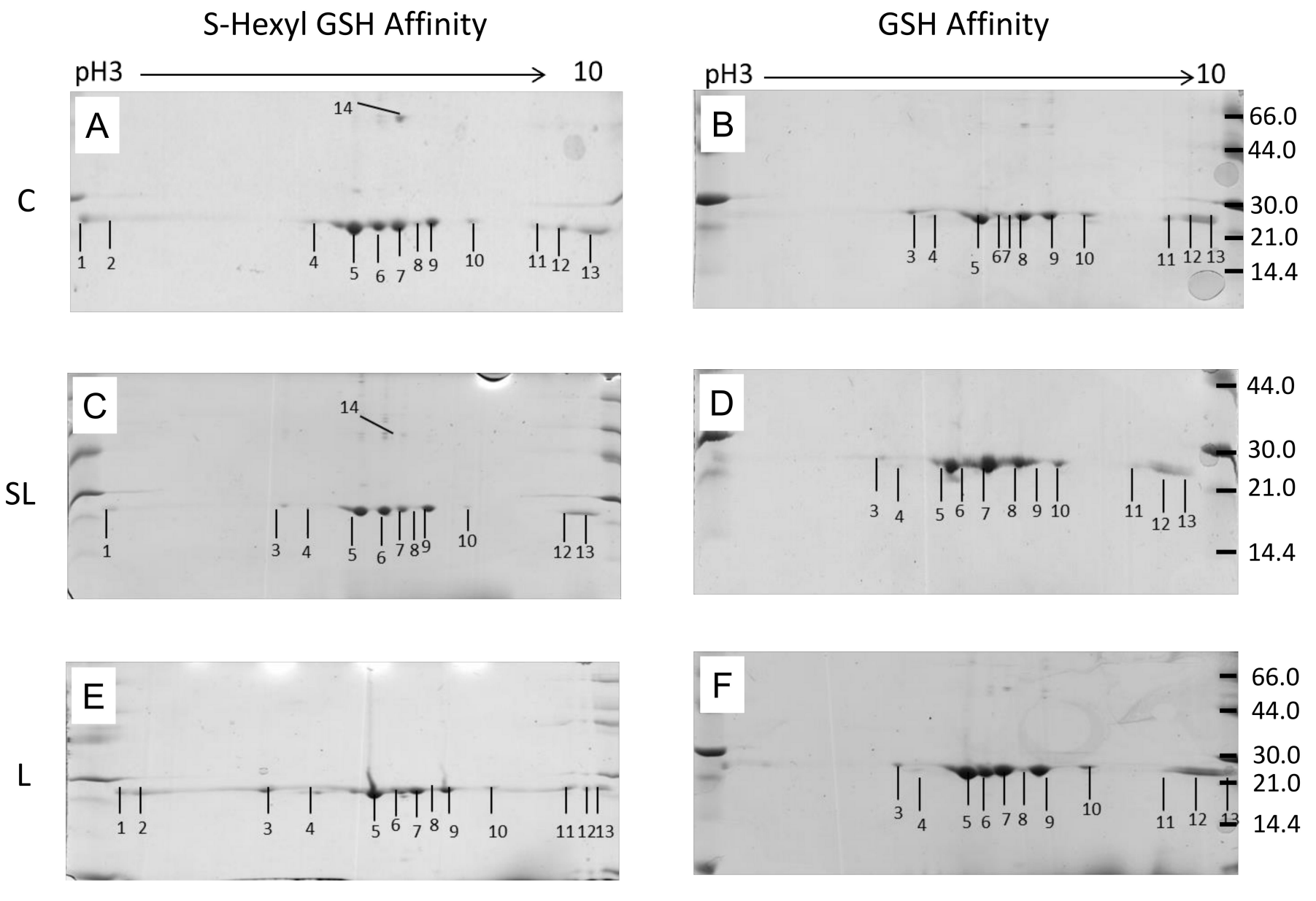
S-Hexyl GSH Affinity
GSH Affinity
pH3
10
pH3
10
A
B
C
D
E
F
C
SL
L
14
1
2
4
5
6
7
8
9
10
11
12
13
3
66.0
44.0
30.0
21.0
14.4

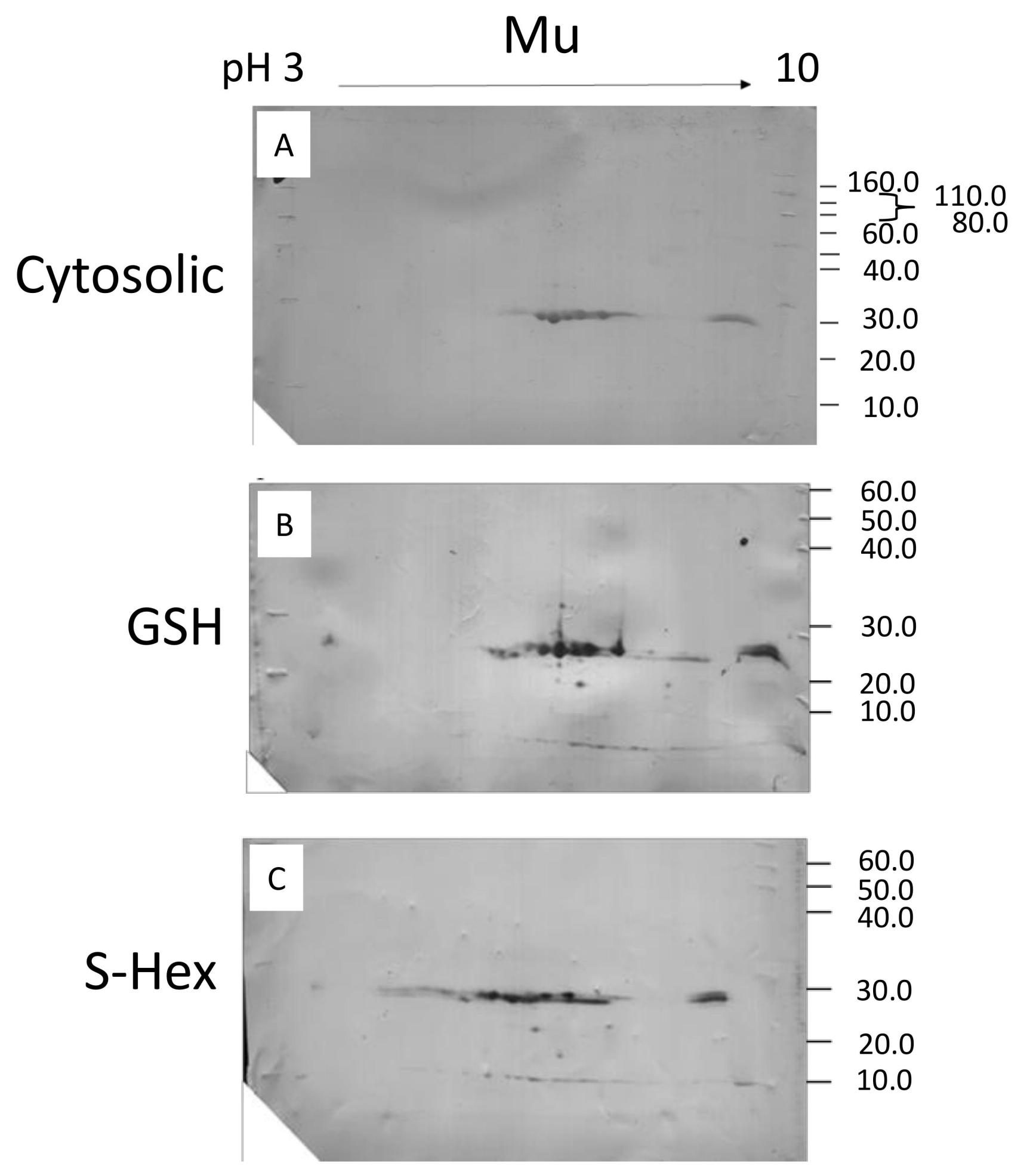
Mu
pH 3
10
A
Cytosolic
160.0
110.0
80.0
60.0
40.0
30.0
20.0
10.0
B
GSH
60.0
50.0
40.0
30.0
20.0
10.0
C
S-Hex
60.0
50.0
40.0
30.0
20.0
10.0

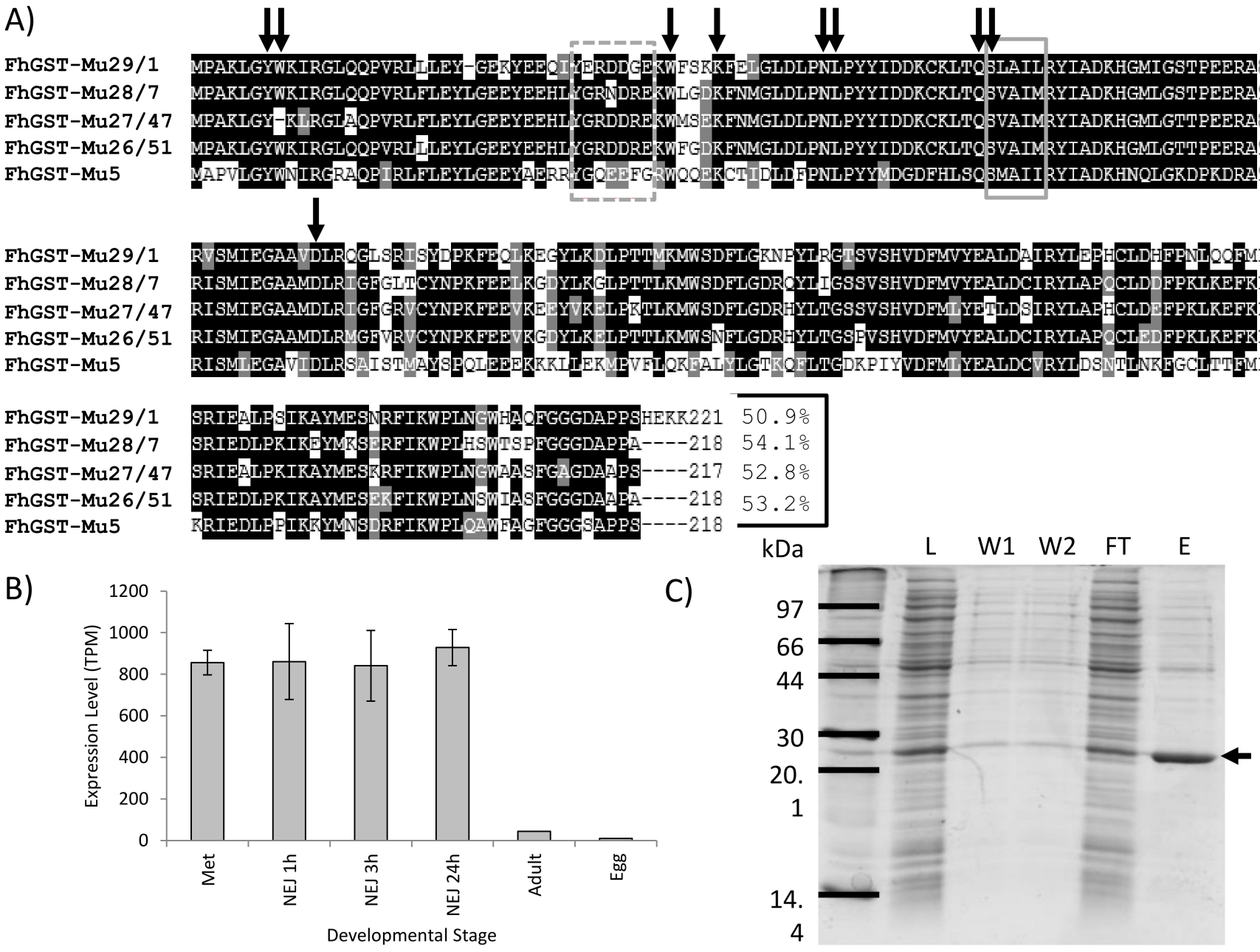
A)
FhGST-Mu29/1
FhGST-Mu28/7
FhGST-Mu27/47
FhGST-Mu26/51
FhGST-Mu5
50.9%
54.1%
52.8%
53.2%
B)
Expression Level (TPM)
1200
1000
800
600
400
200
0
Met
NEJ 1h
NEJ 3h
NEJ 24h
Adult
Egg
Developmental Stage
C)
kDa
L
W1
W2
FT
E
97
66
44
30
20.1
14.4

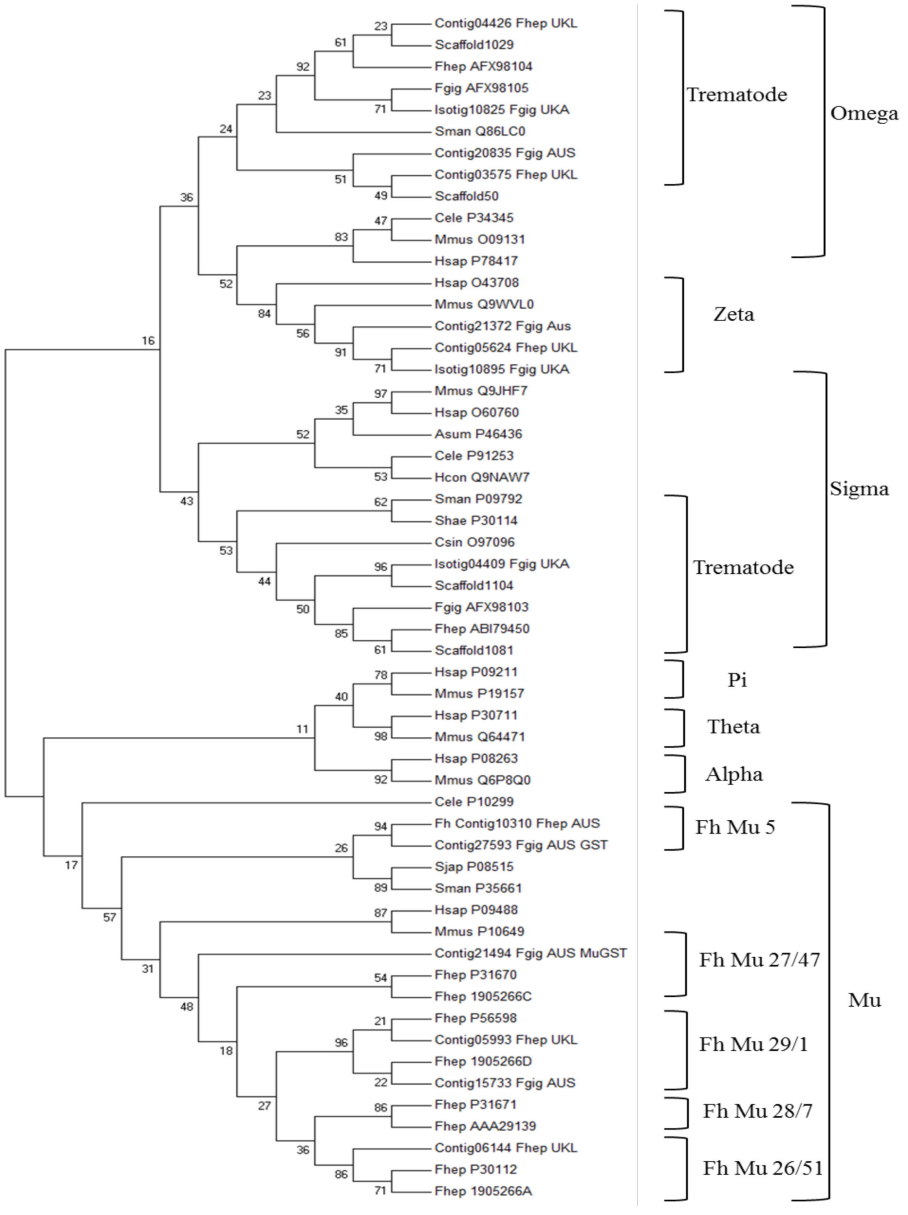
Contig04426 Fhep UKL
Scaffold1029
Fhep AFX98104
Fgig AFX98105
Isotig10825 Fgig UKA
Sman Q86LC0
Contig20835 Fgig AUS
Contig03575 Fhep UKL
Scaffold50
Cele P34345
Mmus O09131
Hsap P78417
Hsap O43708
Mmus Q9WVL0
Contig21372 Fgig Aus
Contig05624 Fhep UKL
Isotig10895 Fgig UKA
Mmus Q9JHF7
Hsap O60760
Asum P46436
Cele P91253
Hcon Q9NAW7
Sman P09792
Shae P30114
Csin O97096
Isotig04409 Fgig UKA
Scaffold1104
Fgig AFX98103
Fhep ABI79450
Scaffold1081
Hsap P09211
Mmus P19157
Hsap P30711
Mmus Q64471
Hsap P08263
Mmus Q6P8Q0
Cele P10299
Fh Contig10310 Fhep AUS
Contig27593 Fgig AUS GST
Sjap P08515
Sman P35661
Hsap P09488
Mmus P10649
Contig21494 Fgig AUS MuGST
Fhep P31670
Fhep 1905266C
Fhep P56598
Contig05993 Fhep UKL
Fhep 1905266D
Contig15733 Fgig AUS
Fhep P31671
Fhep AAA29139
Contig06144 Fhep UKL
Fhep P30112
Fhep 1905266A
Trematode
Omega
Zeta
Sigma
Trematode
Pi
Theta
Alpha
Fh Mu 5
Fh Mu 27/47
Fh Mu 29/1
Fh Mu 28/7
Fh Mu 26/51
Mu